Multitip Near-Field Scanning Thermal Microscopy

Philippe Ben-Abdallah[*]

*Laboratoire Charles Fabry, UMR 8501, Institut d'Optique, CNRS, Université Paris-Saclay,
2 Avenue Augustin Fresnel, 91127 Palaiseau Cedex, France*

A theory is presented to describe the heat flux radiated in the near-field regime by a set of interacting nanoemitters held at different temperatures in vacuum or above a solid surface. We show that this thermal energy can be focused and even amplified in spots that are much smaller than those obtained with a single thermal source. We also demonstrate the possibility to locally pump heat using specific geometrical configurations. These many body effects pave the way to a multitip near-field scanning thermal microscopy that could find broad applications in the fields of nanoscale thermal management, heat-assisted data recording, nanoscale thermal imaging, heat capacity measurements, and infrared spectroscopy of nano-objects.

Heat flux focusing radiated by a hot object at temperature T is limited in the far-field regime by diffraction to $\lambda_{\mathrm{th}}/2$, where $\lambda_{\mathrm{th}} = \hbar c / k_B T$ is the thermal wavelength associated with this source. However, at subwavelength distance from the source the situation can radically change. The near-field scanning thermal microscope (SThM) [1–5], which is the noncontact version of a conventional scanning thermal microscope (STM) [6,7], can achieve local heating at the submicrometric scale with heat sources close to the ambient temperature using the tunneling of nonradiative thermal photons (i.e., evanescent waves). This near-field technology is, among others, the current paradigm of hard-disk-drive writing technology that is based on the so-called heat-assisted magnetic recording [8,9]. In this technique a tiny surface area of a magnetic material is heated up in the near-field regime to raise the material temperature close to its Curie temperature, thus demagnetizing it locally. To store a high density of magnetic bit the hot spot area should be ideally reduced as close as possible as the superparamagnetic limit beyond which the bits become unstable due to thermal fluctuations. The typical size to observe superparamagnetism in usual magnetic materials is typically below domains of 20 nm side. However, the radiative heat focusing by a conventional scanning probe microscope (SPM) is limited by the emission pattern in near-field regime of its tip.

In the present Letter we theoretically investigate the electromagnetic field radiated by a multitip SThM setup (Fig. 1) that consists in several SPM units with tips which are individually positioned using nanopositioning systems based, for instance, on differential interferometry between the tips and thermally controlled with thermocouple junctions inserted inside each tip associated with loops of feedback control. Each single source at temperature T_i is a broadband emitter that radiates over a spectral range

defined by Planck's distribution function at temperature T_i, its maximum being located at the Wien's wavelength $\lambda_{\mathrm{Wi}}(\mu\mathrm{m}) = 2898/T_i(\mathrm{K})$. Hence, for a set of N emitters at different temperatures $T_1 < \ldots < T_N$ we can define N corresponding Wien's wavelengths $\lambda_{WN} < \ldots < \lambda_{W1}$ which set the spectral range $[\alpha\lambda_{WN}, \beta\lambda_{W1}]$ (typically $\alpha \sim 0.1$ and $\beta \sim 100$) within which all heat exchanges occur. We demonstrate that the heat flux radiated by these thermal emitters can be focused and amplified into spots of much smaller area than with a single tip setup. Moreover, we show that this focusing can be achieved up to a surface area close to the superparamagnetic limit. Also we demonstrate with sharp geometric configurations the existence of a near-field heat pumping effect. To highlight those effects and to introduce the basic principles that drive the thermal emission in a multitip SThM platform we consider elongated SPM tips with glass nanospheres ($R = 20$ nm)
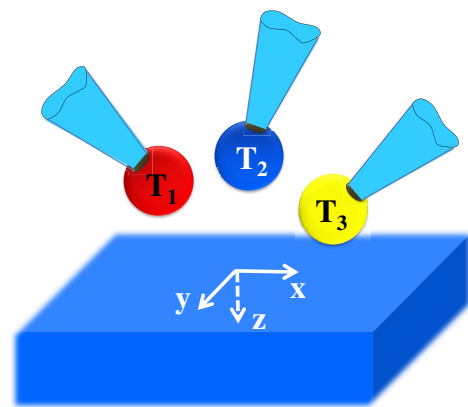

FIG. 1. Schematic of a multitip SThM platform. Nanospheres (thermal emitters) are grafted on single SPM tips. Their temperature and position are individually controlled.

264301-1

attached at their apex. With temperatures close to the ambient temperature the tip radii are extremely small compared with the smallest thermal wavelength so that they act more like dipoles than macroscopic spheres. Hence the multitip SThM platform can be modeled by simple radiating dipoles provided their separation distance is large enough to make the contribution of multipoles negligible. Typically this condition is satisfied [10–12] when the separation distances (center to center) are larger than $3R$. Under these assumptions the optical behavior of any arbitrary multitip setup composed by N tips can be described by the interaction of fluctuating dipoles associated with each nanoemitter. The heat flux radiated through an oriented surface by such a set of emitters held at different temperature T_i can be calculated from the statistical averaging of the Poynting vector spectrum

$$\langle \tilde{\mathbf{S}}(\mathbf{r}, \omega) \rangle = 2\text{Re}\langle \mathbf{E}(\mathbf{r}, \omega) \times \mathbf{H}^*(\mathbf{r}, \omega) \rangle, \quad (1)$$

where the electric and magnetic field can be related to local fluctuating dipoles $\mathbf{p}_i^{\text{fluc}}$ by the following relations [13]:

$$\mathbf{E}(\mathbf{r}, \omega) = \omega^2 \mu_0 \sum_{i=1}^{N} \mathbb{G}^{EE}(\mathbf{r}, \mathbf{r_i}) \mathbf{p_i}^{\text{fluc}}, \quad (2)$$

$$\mathbf{H}(\mathbf{r}, \omega) = -i\omega \sum_{i=1}^{N} \mathbb{G}^{HE}(\mathbf{r}, \mathbf{r_i}) \mathbf{p_i}^{\text{fluc}}, \quad (3)$$

where $\mathbb{G}^{EE}$ and $\mathbb{G}^{HE}$ are the full electric and magnetic dyadic Green's tensors at the frequency ω which take into account all many-body interactions and eventually interactions with an interface [14]. Hence, using the fluctuation dissipation theorem [15]

$$\langle p_{i,\alpha}^{\text{fluc}} p_{j,\beta}^{\text{fluc}*} \rangle = 2 \frac{\epsilon_0}{\omega} \text{Im}(\alpha_i) \Theta(\omega, T_i) \delta_{ij} \delta_{\alpha\beta} \quad (4)$$

(with α_i the polarizability associated with the ith dipole), the spectrum of Poynting components reads

$$\langle \tilde{S}_\zeta(\mathbf{r}, \omega) \rangle = 2 \frac{\omega^2}{c^2} \sum_{i=1}^{N} a_\zeta(\mathbf{r}, \mathbf{r_i}, \omega) \Theta(T(\mathbf{r_i}), \omega), \quad (5)$$

where $\Theta(T, \omega) = \hbar\omega / [e^{[(\hbar\omega)/(k_B T)]} - 1]$ is the mean energy of a harmonic oscillator at temperature T and

$$a_\zeta(\mathbf{r}, \mathbf{r_i}, \omega) \equiv \epsilon_{\zeta\gamma\beta} \text{Im}\{\mathbb{G}_{\beta\eta}^{EE}(\mathbf{r}, \mathbf{r_i}) \mathbb{G}_{\gamma\eta}^{HE*}(\mathbf{r}, \mathbf{r_i})\} \text{Im}(\alpha_i), \quad (6)$$

with summation over the repeated indices γ, β, and η.

To discuss the specificities of the multitip near-field thermal microscopy let us consider a triangular three-tip configuration as depicted in the inset of Fig. 2(a), where all emitters (nanospheres glass) are placed at the apex of an isosceles triangle and are thermalized at the same temperature. We also neglect the far-field heat flux exchanged
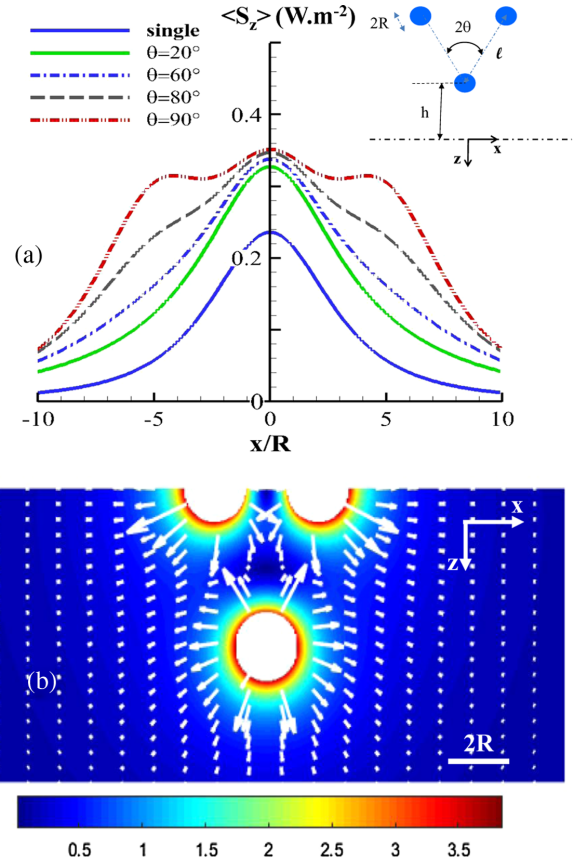

FIG. 2. (a) Normal component $\langle S_z \rangle$ of the Poynting vector radiated through the surface $z = 0$ by a three-tips SThM setup made with nanoemitters in glass [19] held at the same temperature for different angular openings ($T = 300$ K, $R = 20$ nm, $h = 4R$, and $l = 5R$). The blue continuous line corresponds to the case of a single emitter located at $z = -h$. (b) Magnitude of Poynting vector and vector field in the (x, z) plane radiated by a multitip setup of angular opening $\theta = 20°$.

with the external bath in front of the near-field heat flux radiated by the multitip setup in its close neighborhood [16]. This is equivalent to assume an environment at 0 K. The normal component $\langle S_z \rangle = \int [(d\omega)/(2\pi)] \langle \tilde{S}_z(\omega) \rangle$ of the Poynting vector radiated in the near field by this system across the plane $z = 0$ at a distance $h = 4R$ from the lowest apex is shown in Fig. 2(a) for different angular opening θ and compared with the flux radiated by a single emitter at the same distance and same temperature. We consider the system in the steady state regime that is after a thermalization time, which is typically, for many-body systems, of the order of the millisecond [17]. With this thermalized system the FWHM of heat flux trivially increases with θ and it is always greater than with a single emitter. This behavior is simply due to the fact that the emission pattern of the whole structure corresponds to the superposition of flux radiated by three fluctuating dipoles with the same distribution function and with a polarizability equal to its dressed polarizability to take into account the cooperative

effects. In the near-field regime we see [Fig. 2(b)] that the flux lines diverge from the source in a similar way as around a single object. In the far-field regime (i.e., $\text{Min}_i|\mathbf{r} - \mathbf{r_i}| \gg \lambda_{th}$) the thermal emission can be calculated using Kirchoff's law from the absorption cross section of the system which reduces after a straightforward calculation using the Landauer formalism [18] to

$$\sigma_a(\omega) = 4\pi A(\mathbf{u})| \sum_{i=1}^{N} \mathbf{a}(\mathbf{r}, \mathbf{r_i}, \omega).\mathbf{u}|, \qquad (7)$$

with $A(\mathbf{u})$ being the apparent surface of the system in the direction $\mathbf{u}$ along which it is shined.

On the contrary, for a system out of thermal equilibrium, the situation radically changes. In particular Kirchoff's law fails to describe its thermal behavior in the far-field regime since according to expression (5) light emission and therefore light absorption is no longer an intrinsic property of the system but it closely depends on its local thermal state, that is, on its temperature. Hence we see in Fig. 3 by heating up the base of the triangular system that the heat flux can be focused on a much smaller spot than with a fully thermalized system (Fig. 2). In this case the FWHM of the heat flux profile at $z = 0$ can even be between 1.5 to 2 times smaller than with a single tip depending on the angular opening of the multitip setup. It is worthwhile to note that the heat flux is enhanced by approximately 2 orders of magnitude compared to a thermalized system of three dipoles or a single emitter when the triangle base is heated up by only 50 K.

We also observe in Fig. 3(a) that for systems with a small angular opening the heat flux can back propagate toward the emitting system itself just below the cold tip while it flows toward the surrounding environment around this region, showing so that a multitip setup can be used as a local heat pump. On the other hand, for large angular openings, this pumping effect is off center. The mapping of the Poynting vector field [Fig. 3(b)] in the (x, z) plane shows that this effect results from the local bending of flux lines. The mechanism responsible for the redirection of energy flow toward the system is directly related, according to expression (5), to the presence of a local temperature difference inside the system. The consequences of this gradient on the heat pumping and focusing effects are highlighted in Fig. 3(c) in the case of a triangular system subject to two temperature differences between its apex and its base. We see that the magnitude of those effects depends directly on this temperature discrepancy. In particular we observe that while this magnitude increases when the thermal emission of the apex particle is reduced, the presence of this particle is nevertheless fundamental for these effects to exist. Indeed we see in Fig. 3(c) that without this particle the magnitude of heat flux falls down by approximately 2 orders of magnitude. Hence, even if the
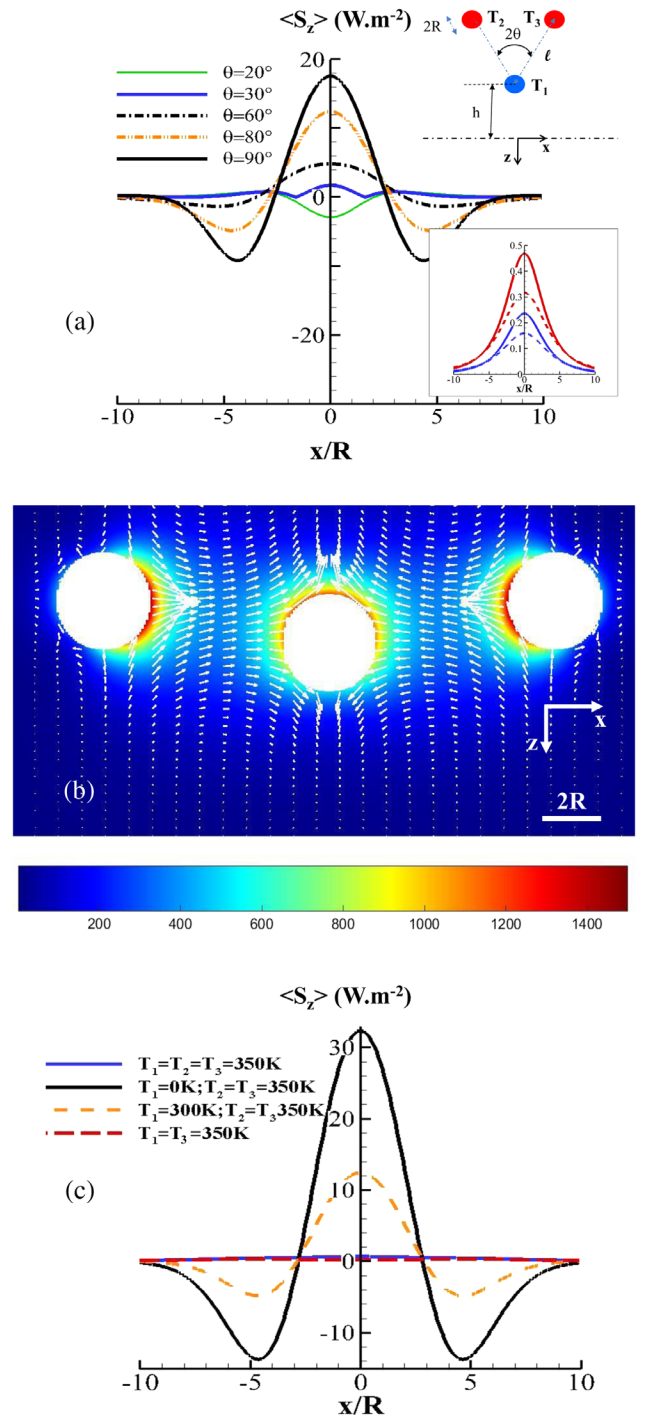

FIG. 3. (a) Normal component $\langle S_z \rangle$ of the Poynting vector radiated through the surface $z = 0$ by a three-tip SThM setup made with three glass emitters held at $T_2 = T_3 = 350$ (red) and $T_1 = 300$ K (blue) for different angular opening ($R = 20$ nm, $h = 4R$, and $l = 5R$). The inset shows the flux at $z = 0$ for a single particle at $T = 350$ (red) and $T = 300$ K (blue) at $z = 4R$ (solid) and $z = 4R + l\cos(80)$ (dashed). (b) Magnitude of the Poynting vector and vector field in the (x, z) plane radiated by a multitip setup of angular opening $\theta = 80°$. (c) Normal component $\langle S_z \rangle$ of the Poynting vector at $z = 0$ with respect to the temperature differences. The long dashed red line corresponds to the flux emitted by two particles (2 and 3) at the same temperature.

apex particle is nonemitting ($T = 0$ K) it participates both with the local heat funneling (heat pumping and heat focusing) by distorting the flux lines and to the exaltation by the dressing effect of the thermal emission in the near-field regime of two others particles.

The above analysis holds when the overall system is in vacuum. In the following we discuss how the highlighted effects are impacted by the presence of an interface. To do so, we consider similar dipolar systems held close to the ambient temperature which are brought, at subwavelength distances, from a simple silicon (Si) sample. In the spectral range where most of the heat exchanges take place the dielectric permittivity of Si is close to $\epsilon_{Si} = 11.5$ [19]. In Fig. 4 we show the heat flux radiated by a triangular system made of glass nanoparticles [Fig. 4(a)] and of gold nanoparticles [Fig. 4(c)], respectively. The results show that, for polar particles, the heat flux is amplified by more than a factor when the particles are parallel to the surface compared to the same configuration in vacuum. The flux is even amplified by almost a factor 4 for an angular opening of $\theta = 80°$. On the other hand, for metallic particles [Fig. 4(c)] the amplification factor remains smaller than the two highlighting, so the important role played by the resonant modes (surface phonon polaritons) is supported by the glass particles. As the focusing effect is concerned it is slightly improved by the presence of the interface when $\theta = 80°$. Indeed, in this case the FWHM $= 3.34R$ while for a single particle FWHM$_{single} = 3.9R$. In Fig. 4(b) we see that this focusing evolves nonmonotonically with the nanoparticles' radius. It is worthwhile to note that the FWHM for a multitip setup is always smaller than with a single tip when $R > 20$ nm (for large particles the contribution of the magnetic moment should also be taken into account and would required further investigations). For small particles the FWHM can be comparable to the superparamagnetic limit of the usual recording materials [20,21]. In this case the focusing is not necessarily better than with a single particle, but the heat flux can be 10 times more important than with a single emitter. However, the optimization of the focusing effect with respect to the geometrical configuration, the materials properties, and the temperature distribution remain today open problems which go far beyond the scope of the present Letter.

In summary, we have introduced the concept of multitip near-field scanning thermal microscopy and demonstrated that it can be used to tailor heat flux at the nanoscale. We have shown that this flux can be focused and even amplified in tiny regions that are much smaller than the diffraction limit and even smaller than with a single tip near-field SThM. The relatively simple model used to describe the tips does not allow us to setup with tips close to the contact. For such separation distances the dipolar approximation fails to describe properly the thermal behavior of emitters and the higher order modes have to
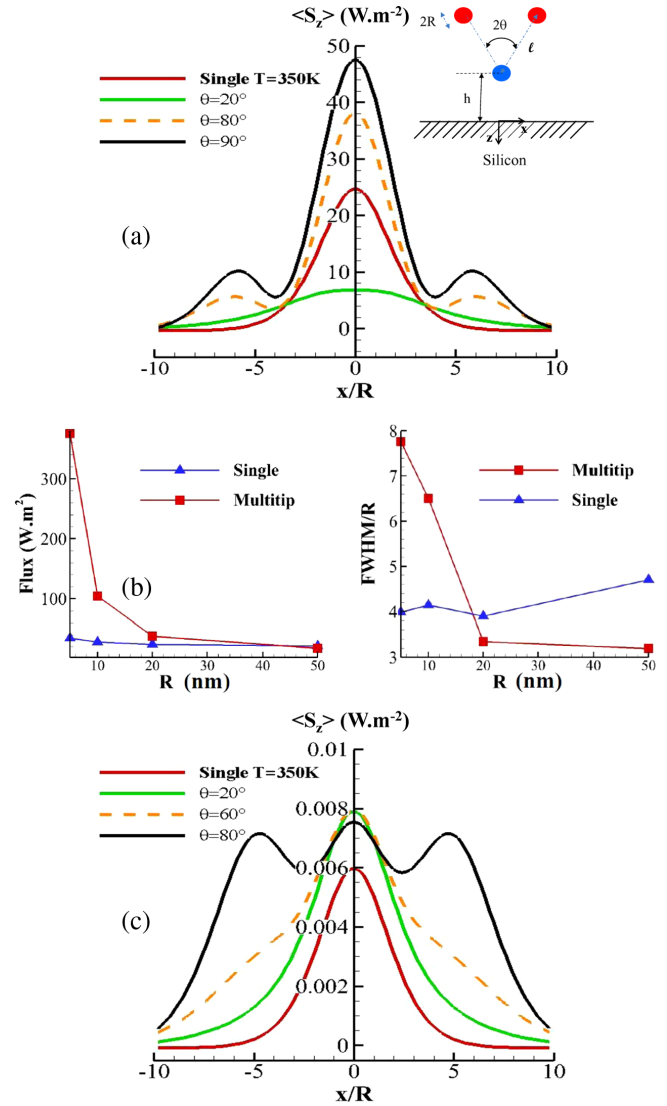

FIG. 4. Normal component $\langle S_z \rangle$ of the Poynting vector radiated through the surface $z = 0$ by three (a) glass nanoparticles above a silicon sample (same parameters as in Fig. 3). The red curve shows the flux at $z = 0$ for a single particle at $T = 350$ K located at $z = 4R$ above the silicon sample. (b) $\langle S_z \rangle$ at $z = 0$ and $x = 0$ and FWHM for different radius with an angular opening of $\theta = 80°$. (c) Same as (a) with gold nanoparticles.

be taken into account. These modes give a supplementary degree of freedom to sculpt the field radiated by the sources and we can expect even better performances with such configurations. The significance of multitip scanning thermal microscopy to analyze at nanoscale the thermal state of solid surfaces is obvious. It could also find broad applications in many other fields to measure, for instance, thermal properties such as heat capacity and the infrared spectra of nano-objects.

*pba@institutoptique.fr

[1] Y. De Wilde, F. Formanek, R. Carminati, B. Gralek, P. Lemoine, K. Joulain, J. Mulet, Y. Chen, and J. J. Greffet, Nature (London) **444**, 740 (2006).

[2] A. Kittel, U. F. Wischnath, J. Welker, O. Huth, F. Ruting, and S.-A. Biehs, Appl. Phys. Lett. **93**, 193109 (2008).

[3] A. C. Jones and M. B. Raschke, Nano Lett. **12**, 1475 (2012).

[4] F. Huth, M. Schnell, J. Wittborn, N. Ocelic, and R. Hillenbrand, Nat. Mater. **10**, 352 (2011).

[5] Q. Weng, S. Komiyama, L. Yang, Z. An, P. Chen, S.-A. Biehs, Y. Kajihara, and W. Lu, Science **360**, 775 (2018).

[6] C. C. Williams and H. K. Wickramasinghe, Appl. Phys. Lett. **49**, 1587 (1986).

[7] A. Majumdar, J. Lai, M. Chandrachood, O. Nakabeppu, Y. Wu, and Z. Shi, Rev. Sci. Instrum. **66**, 3584 (1995).

[8] W. A. Challener *et al.*, Nat. Photonics **3**, 220 (2009).

[9] B. C. Stipe *et al.*, Nat. Photonics **4**, 484 (2010).

[10] P. Ben-Abdallah, K. Joulain, J. Drevillon, and C. Le Goff, Phys. Rev. B **77**, 075417 (2008).

[11] A. Pérez-Madrid, J. M. Rubi, and L. C. Lapas, Phys. Rev. B **77**, 155417 (2008).

[12] D. Becerril and C. Noguez, Phys. Rev. B **99**, 045418 (2019).

[13] P. Ben-Abdallah, S.-A. Biehs, and K. Joulain, Phys. Rev. Lett. **107**, 114301 (2011).

[14] See Supplemental Material at http://link.aps.org/supplemental/10.1103/PhysRevLett.123.264301 for the expressions of the full Green's tensors in vacuum and in the presence of an interface.

[15] H. B. Callen and T. A. Welton, Phys. Rev. **83**, 34 (1951).

[16] V. Yannopapas and N. V. Vitanov, Phys. Rev. Lett. **110**, 044302 (2013).

[17] R. Messina, M. Tschikin, S.-A. Biehs, and P. Ben-Abdallah, Phys. Rev. B **88**, 104307 (2013).

[18] S.-A. Biehs and P. Ben-Abdallah, Phys. Rev. B **93**, 165405 (2016).

[19] *Handbook of Optical Constants of Solids*, edited by E. Palik (Academic Press, New York, 1998).

[20] D. Weller and A. Moser, IEEE Trans. Magn. **35**, 4423 (1999).

[21] D. A. Thompson and J. S. Best, IBM J. Res. Dev. **44**, 311 (2000).